sustainability

MDPI

Article

A Multi-Temporal Analysis on the Dynamics of the Impact of Land Use and Land Cover on NO_2 and CO Emissions in Argentina for Sustainable Environmental Management

Viviana Fernández-Maldonado [1,2,†], Ana Laura Navas [1,†], María Paula Fabani [1,3], Germán Mazza [4] and Rosa Rodríguez [1,*]

[1] Grupo Vinculado al PROBIEN (CONICET-UNCo), Instituto de Ingeniería Química, Facultad de Ingeniería, Universidad Nacional de San Juan, Av. Libertador San Martín (Oeste) 1109, San Juan J5400ARL, Argentina; vivifernandezm@unsj-cuim.edu.ar (V.F.-M.); analauranavas@gmail.com (A.L.N.); paufabani@unsj.edu.ar (M.P.F.)
[2] Observatorio de Cambio Climático de San Juan, Secretaria de Ambiente y Desarrollo Sustentable, Gobierno de la Provincia de San Juan, Calle 5 y Pelegrini, Al Pie del Cerro Parkison, San Juan J5400ARL, Argentina
[3] Instituto de Biotecnología, Facultad de Ingeniería, Universidad Nacional de San Juan, Av. Libertador San Martín (Oeste) 1109, San Juan J5400ARL, Argentina
[4] Instituto de Investigación y Desarrollo en Ingeniería de Procesos, Biotecnología y Energías Alternativas, PROBIEN (CONICET-UNCo), Calle Buenos Aires, 1400, Neuquén Q8300IBX, Argentina; german.mazza@probien.gob.ar
* Correspondence: rrodri@unsj.edu.ar
† These authors contributed equally to this work.

Abstract: This study presents an analysis of NO_2 and CO emissions in Argentina, utilizing remote sensing data. This research aims to determine the spatiotemporal distribution of NO_2 and CO emissions from 2019 to 2021. It examines the influence of land use and cover on NO_2 and CO emissions using various climatic, anthropic, and natural indicators. The year with the highest CO and NO_2 concentration was 2020. NO_2 exhibited the highest concentrations in built-up urban areas and croplands, notably impacting the capital city and the northern region of Buenos Aires province. Also, CO concentration was influenced by anthropic variable distances to national route, mining extraction, power plants, airports, and urban index (UI). They were also influenced by climatic and natural variables (Palmer drought index, vapor pressure, maximum environment temperature, wind speed, DEM, humidity, and normalized difference vegetation index (NDVI)) for the different uses and land covers. NO_2 concentrations were influenced by anthropic (distance to airports, service stations, open dumpsites, power plants, and factories), climatic, and natural variables (Palmer drought index, vapor pressure, wind speed, and DEM) for the different uses and land cover. This research supports sustainable environmental management by guiding the development of effective emission mitigation strategies for improved community health and well-being.

Keywords: atmospheric pollution; remote sensing data; land uses and land cover; gases; environmental management

check for updates

Citation: Fernández-Maldonado, V.; Navas, A.L.; Fabani, M.P.; Mazza, G.; Rodríguez, R. A Multi-Temporal Analysis on the Dynamics of the Impact of Land Use and Land Cover on NO_2 and CO Emissions in Argentina for Sustainable Environmental Management. *Sustainability* **2024**, *16*, 4400. https://doi.org/10.3390/su16114400

Academic Editor: Mohammad Aslam Khan Khalil

Received: 9 April 2024
Revised: 12 May 2024
Accepted: 18 May 2024
Published: 23 May 2024

Copyright: © 2024 by the authors. Licensee MDPI, Basel, Switzerland. This article is an open access article distributed under the terms and conditions of the Creative Commons Attribution (CC BY) license (https://creativecommons.org/licenses/by/4.0/).

1. Introduction

Air quality is an increasingly relevant issue on the global agenda, supported by recognition in the United Nations sustainable development goals (SDGs). These goals, addressing health, energy, and sustainable urban development, are linked to the issue of air pollution [1]. Air pollution is considered the world's greatest environmental health threat, causing 7 million deaths worldwide each year [2]. Exposure to air pollutants is the most critical risk factor for major non-communicable diseases [3]. In a context where air quality has become a critical factor for public health, it is alarming to note that outdoor air pollution contributed to 4.2 million deaths worldwide in 2016 according to the World Health

Organization [4]. These staggering figures reveal that air pollution is a global challenge deeply affecting human health. The WHO assessment indicates that this pollution is responsible for 29% of lung cancer deaths, 43% of chronic obstructive pulmonary disease (COPD) deaths, approximately 25% of deaths from ischemic heart disease, and 24% of deaths from strokes globally [5].

This environmental issue knows no borders, and Argentina is no exception. Air pollution in the country is a topic deserving increasing attention. Its main causes are diverse, ranging from economic development and urbanization to energy consumption, transportation, and rapid urban population growth [6]. Two key indicators of air quality, nitrogen dioxide (NO_2) and carbon monoxide (CO), pose significant hazards to human health and the environment [7]. Therefore, it is imperative to periodically monitor and reduce atmospheric pollutant concentrations to mitigate their harmful consequences.

Nitrogen dioxide (NO_2) plays a crucial role in atmospheric chemistry, air quality, and climate change, acting as an indirect greenhouse gas contributing to global warming [8]. NO_2 originates from both natural sources and human activity, with fossil fuel combustion being the predominant source. Its presence in urban areas, where multiple emission sources and dense populations are concentrated, further exacerbates health risks. Meanwhile, carbon monoxide (CO), another critical pollutant, is primarily released through incomplete combustion of fossil fuels and industrial processes, making it a significant concern for public health [9]. Forest fires are a source of many air pollutants in the atmosphere. During such events, significant amounts of carbon monoxide (CO) and nitrogen oxides such as NO, NO_2, methane (CH_4), and non-methane hydrocarbons (NMHCs) are released. Their emissions significantly disrupt the chemical climate on local, regional, and global scales [10]. They chemically produce ozone, a secondary pollutant, which is an oxidizing agent and a greenhouse gas with potential climate implications [10].

Land use and land cover change (LULCC) are fundamental factors influencing environmental dynamics and atmospheric emissions worldwide [11]. Land cover refers to the surface class covering the land, such as forests, grasslands, urban areas, etc., while land use refers to how the land is used, such as agriculture, urbanization, industry, etc. Land use/cover change (LULCC) has become one of the key elements in global environmental change and sustainable development [12,13]. This is due to its omnipresence at the local scale and its globally recognized environmental impact [11,14]. The intensification of agricultural and industrial activities driven by rapid population growth has led to significant changes in LULC (land use/land cover) and increased demands on natural resources housed in the land [11,14]. In recent decades, an exhaustive analysis of urban expansion has been carried out worldwide to understand how coverage changes can affect the sustainable development of cities [13,14]. In Argentina, a country known for its diverse ecosystems and extensive agricultural landscapes, understanding the intricate relationship between land use patterns and emissions of nitrogen dioxide (NO_2) and carbon monoxide (CO) is crucial for sustainable environmental management.

As noted by Le et al. [15], the intricate interaction between land use changes and atmospheric emissions requires a multi-temporal analysis to unravel the dynamics shaping environmental impacts. This aspect resonates with the urgent need for comprehensive assessments, as echoed by Ooi et al. [16], to effectively mitigate the consequences of land use alterations on air quality and atmospheric composition. Despite the importance of understanding and monitoring these trace gases, research on NO_2 and CO in the region of South America is limited, adding to the lack of air quality monitoring stations in many Latin American countries. However, in recent decades, the availability of satellite observations, such as the tropospheric monitoring instrument (TROPOMI) aboard the Copernicus Sentinel-5 Precursor (S5P) satellite, has allowed unprecedented access to NO_2 and CO measurements with global spatial coverage [17].

In this context, this study aims to investigate the multi-temporal dynamics of NO_2 and CO emissions in Argentina, driven by changes in land use and cover, using a robust methodology integrating remote sensing techniques and atmospheric modeling. The in-

sights gained will enhance understanding of spatiotemporal emission patterns and provide guidance for sustainable environmental management practices. By analyzing these emissions over three years (2019–2021), this study aims to identify the spatial distribution and behavioral patterns of CO and NO_2 and determine their impact factors on land use/cover (LULC). Despite the short duration of this period, possible trends will be explored to shed light on the evolution of these pollutants in the region. This study is essential for better understanding environmental risks and health associated with air quality in Argentina and may lay the groundwork for future policies and mitigation measures.

2. Materials and Methods

2.1. Study Area

Argentina occupies the southern tip of South America between parallels 22 and 56 south, with wide access to the Atlantic Sea. This study's area is composed of 23 provinces and the autonomous city of Buenos Aires, the capital of the country, with a total area of 2,780,400 km^2 (Figure 1). It is the second largest country in South America and the eighth largest in the world. The climate of Argentina is determined by its latitudinal extension, encompassing warm subtropical climates in the north, temperate climates in the central east, arid climates that cross the country from north to south, and cold climates in the south [https://www.ign.gob.ar/ (accessed on 4 January 2021)]. Its relief is predominantly plain, except in the west of the country along the Andes Mountain range, where the highest altitudes in America are reached (Aconcagua 6960 m). The country's population, according to the preliminary result of the 2022 census, is 45,892,285 habitants (https://censo.gob.ar/index.php/datos_definitivos_total_pais/ (accessed on 25 November 2023)). In Argentina, the primary sources of atmospheric pollution are energy (50.7%), agriculture, livestock, forestry, and other land uses (39.1%), industrial processes and product use (5.7%), and waste (4.5%). Housing contributes an average of 29% of emissions. CO_2 emissions in 2021 reached 366 megatons, ranking Argentina as the 155th country in terms of CO_2 emissions [https://www.argentina.gob.ar/sites/default/files/iea2021_digital.pdf (accessed on 21 December 2022)].

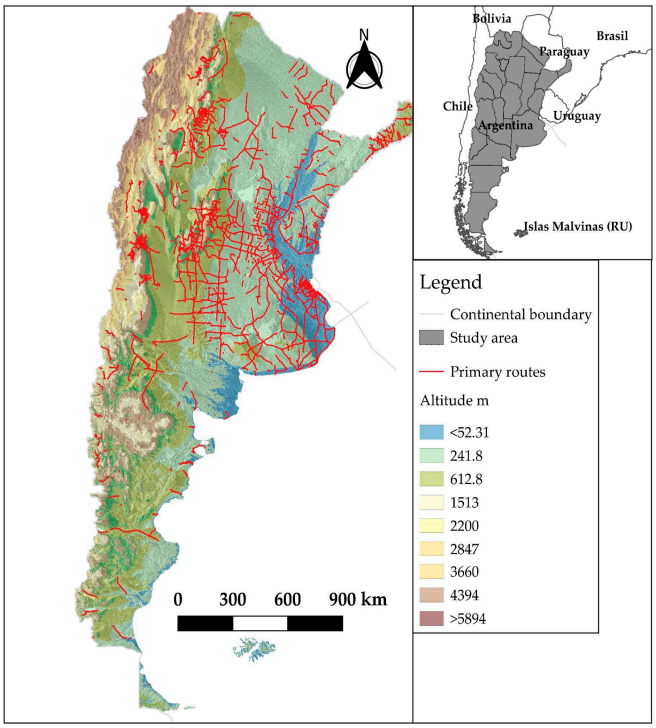


Figure 1. Study area. The Argentine Republic, with an elevation model and most traveled routes.

2.2. Data and Preprocessing

In this study, various spatial data from satellite remote sensing and existing geospatial data were used. In particular, these included air quality data and data that described natural, climatic, and urban indicators. Due to the input data having different resolutions, 1 km was chosen as the uniform spatial unit. In addition, 100 random polygons were taken for each land use and cover for the years 2019, 2020, and 2021. The centroid of the polygon was then extracted and a total of 800 points per year were obtained (see Figure A1). The samples extracted from the year 2021 were used to make the models of objective 2. Furthermore, the area occupied by each polygon was extracted. The methodological flow is illustrated in Figure 2. The LULC maps were obtained from the European Space Agency (ESA) World Cover based on Sentinel-1 and Sentinel-2 data for the years 2019–2021. The global land cover map for the year 2019 had a spatial resolution of 100 m, while the global land cover map for the years 2020 and 2021 had a spatial resolution of 10 m. Because the LULC maps presented different spatial resolutions, they were resampled to a resolution of 1000 m. To see in detail the classification method used, as well as the accuracy of the maps, it is suggested seeing the following links (https://zenodo.org/records/3938968 (accessed on 5 April 2024), https://esa-worldcover.org/en/data-access (accessed on 1 February 2022)). The land cover classes selected were:

- Tree cover: this class includes any geographic area dominated by trees with a cover of 10% or more.
- Shrubland: this class includes any geographic area dominated by natural shrubs having a cover of 10% or more.
- Grassland: this class includes any geographic area dominated by natural herbaceous plants (plants without persistent stems or shoots above ground and lacking definite firm structure) (grasslands, prairies, steppes, savannahs, pastures) with a cover of 10% or more.
- Cropland: land covered with annual cropland that is sown/planted and harvestable at least once within the 12 months after the sowing/planting date.
- Built-up: Land covered by buildings, roads, and other manmade structures such as railroads. Buildings include both residential and industrial buildings. Urban green (parks, sports facilities) is not included in this class. Waste dump deposits and extraction sites are considered bare.
- Bare/sparse vegetation: land with exposed soil, sand, or rocks that never has more than 10% vegetated cover during any time of the year.
- Permanent water bodies: This class includes any geographic area covered for most of the year (more than 9 months) by water bodies, e.g., lakes, reservoirs, and rivers. Can be either fresh or salt water bodies. In some cases, the water can be frozen for part of the year (less than 9 months).
- Herbaceous wetland: land dominated by natural herbaceous vegetation (cover of 10% or more) that is permanently or regularly flooded by fresh, brackish, or salt water.

2.2.1. TROPOMI Product

In the first step of this study, the product offline stream of the NO_2 total column and the CO column from satellite TROPOMI (tropospheric monitoring instrument) was used to extract the median annual NO_2 and CO emissions for the period from January 2019 to December 2021. The spatial resolution of the image was 1113.2 m. Using Engine Code Editor, pollution parameter maps (CO and NO_2) were extracted. Using filters, this study's years and location (country Argentina) were defined. Following that, images with clouds were filtered by defining cloud filters and median filters. The data were downloaded and processed using the QGIS software version 3.22.

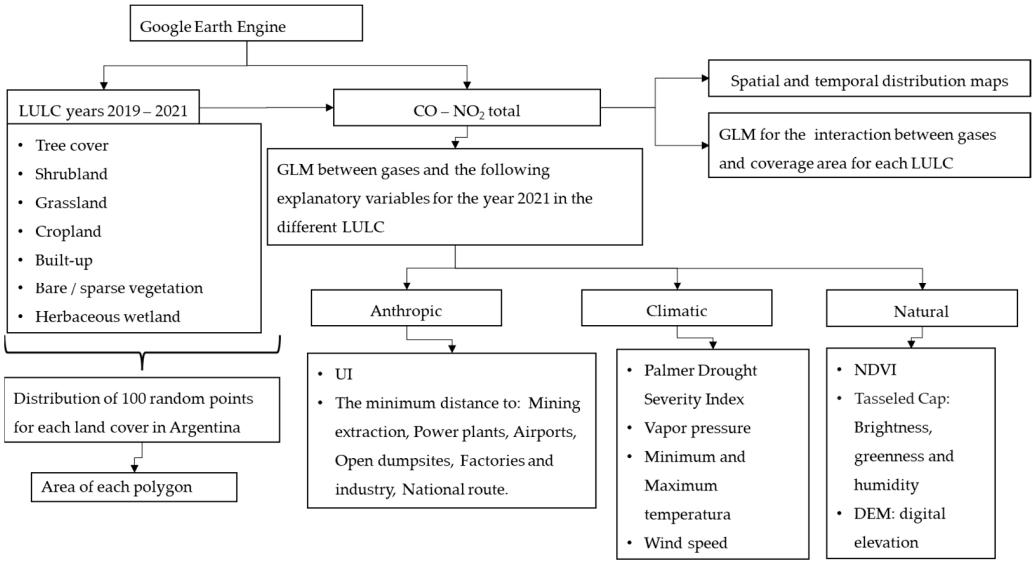


Figure 2. Methodological flow.

2.2.2. Anthropic Indicators

UI (urban index) is an indicator of built-up areas [18] and was obtained using the following equation (Equation (1)):

$$UI = SWIR2\ (Band12) - NIR(Band8a) / SWIR2\ (Band12) + NIR\ (Band8a), \quad (1)$$

UI highlights urban areas with higher reflectance in the shortwave infrared (SWIR2) region compared with the near infrared (NIR) region. The UI value ranged from −1 to +1. Values close to 1 indicated a high density of built-up areas. The UI was developed to map urban areas used to investigate urban density and socio-economic variables. Additionally, this index can detect areas of bare soil [19].

To extract the following variables, the minimum distance from the centroid of each polygon to the following vector layers was taken: mining extraction, power plants, airports, open dumpsites, service stations, factories/industry, and national routes. The layers were downloaded from the National Geographic Institute of the Argentine Republic [https://www.ign.gob.ar/NuestrasActividades/InformacionGeoespacial/CapasSIG (accessed on 15 November 2023)].

2.2.3. Climatic Indicators

The climatic variables were extracted from TerraClimate. This is a high-spatial-resolution (~4 km) gridded dataset of monthly climate and hydroclimate for global land surfaces from 1958 to the present. This dataset is updated annually (https://www.climatologylab.org/datasets.html (accessed on 20 November 2023)) [20]. All variables obtained were resampled to a scale of 1000 m. Then, the annual average of each variable was extracted.

- Palmer drought index: The index uses precipitation and environment temperature data to study moisture supply and demand using a simple water balance model. Negative values indicate droughts and positive values indicate wet areas.
- Vapor pressure (kPa).
- Max and min environment temperature (°C).
- Wind speed (m/s).

2.2.4. Natural Indicators

The NDVI and tasseled cap variables were extracted using Sentinel-2 imagery. These were processed by applying a filter and mask of clouds less than 10%. Then, the median values for each year were extracted.

- NDVI (normalized difference vegetation index) is based on the reflectance of the NIR wave in healthy plants and on the reflectance of the red wave to detect less healthy plants. This index is defined by values ranging from −1 to 1.

$$\text{NDVI} = \text{NIR (Band8)} - \text{RED (Band4)}/\text{NIR (Band8)} + \text{RED (Band4)} \quad (2)$$

- Tasseled cap is a transformation of the information contained in the bands that generates new axes that maximize the information. This is a compression method to reduce multiple spectral data, specifically 6 bands, into a few bands, which allows understanding important phenomena of crop development in spectral spaces.
- Brightness: low brightness values in coincidence with forested areas or, in general, with vegetation cover or bodies of water.

$$\begin{gathered}\text{Brightness} = \text{Band2} \times 0.3029 + \text{Band3} \times 0.2786 + \text{Band4} \times 0.4733 + \\ (\text{Band8} \times 0.5599 + \text{Band11} \times 0.508 + \text{Band12} \times 0.1872\end{gathered} \quad (3)$$

2. Greenness is related to plant masses and bodies of water.

$$\begin{gathered}\text{Greenness} = \text{Band2} \times (-0.2941) + \text{Band3} \times (-0.243) + \text{Band4} \times (-0.5424) + \\ \text{Band8} \times 0.7276 + \text{Band11} \times 0.0713 + \text{Band12} \times (-0.1608)\end{gathered} \quad (4)$$

3. Humidity is related mainly to bodies of water, but also the moisture content of vegetation and soils.

$$\begin{gathered}\text{Humidity} = \text{Band2} \times 0.1511 + \text{Band3} \times 0.1973 + \text{Band4} \times 0.3283 + \\ \text{Band8} \times 0.3407 + (\text{Band11} \times (-0.7117) + \text{Band12} \times (-0.4559)\end{gathered} \quad (5)$$

4. DEM: this SRTM V3 product (SRTM Plus) is provided by NASA JPL at a resolution of 1 arc-second (approximately 30 m).

2.3. Statistical Analysis

Descriptive statistics for the spatiotemporal distribution of CO and NO_2 gases were performed. Additionally, GLMs (generalized linear models) with gamma distribution between the gases and the interaction between the different LULC coverage and the area of each sampled polygon were made (Figure A2). Spatial autocorrelation between polygons was evaluated through the nearest neighbor method. Then, the variance inflation factor (VIF) for any remaining collinearity on the full models from different sets and excluded variables with VIFs > 5 was assessed, which indicated collinearity between predictors [21]. For objective 2, generalized linear models with Gamma distribution only for the data from the year 2021 were performed. Some cover classes were regrouped because they presented similar values in CO and NO_2 concentrations, e.g., tree cover/herbaceous wetland, shrubland/grassland, and cropland/built-up (see Figures A3–A6). The permanent water bodies class is explained in the models. The CO and NO_2 concentrations were related to different predictor variables classified as anthropic, climatic, and natural (see Section 2.2). For each full model, a backward elimination procedure was used to remove no significant variables without losing important information (significance level p-value > 0.05 can be eliminated) and to obtain the minimal adequate model [22]. A pseudo-R^2 was estimated from the deviance values of the best models [23]. To identify collinearity between independent variables, the Pearson correlation method was used [24]. When the coefficient r was $> |0.7|$, variables were excluded. All statistical analyses were carried out using R Core Team (2016).

3. Results and Discussion

3.1. Spatiotemporal Distribution of CO and NO_2 in Argentina during the Years 2019, 2020, and 2021

The results of the annual spatiotemporal distribution of CO and NO_2 in Argentina are presented in Figures 3 and 4. According to Table 1 and Figure 3, the CO concentration

presented its highest values for the year 2020, obtaining similar values for the years 2019 and 2021. These results differed from those found in other countries, since several authors claimed that CO emissions decreased during the 2020 confinement due to the COVID-19 pandemic [25–27]. Although the pandemic may have had a significant impact on some human activities and therefore CO emissions, other factors could have influenced CO emissions during that period. One of the possible reasons could be due to changes in industrial activity. That is to say, even though the pandemic reduced most activities (industrial and commercial), some essential product industries continued to operate normally or even increased their production due to the strong demand for certain products. Another explanation could be due to changes in transportation patterns. Although vehicle traffic was reduced due to the confinement measures, some sectors, such as the transportation of food and essential goods, increased their activity, which could have offset the reductions in other sectors. In summary, it is important to consider several factors when analyzing carbon monoxide (CO) emissions in a country over a specific period, such as the impact of the COVID-19 pandemic on emissions. While the COVID-19 pandemic could have had a significant impact on some activities and therefore CO emissions, there are also other factors to consider when analyzing total CO emissions over a specific period. A comprehensive analysis that takes all of these factors into account is essential to fully understand CO emissions trends in a country over a given period.

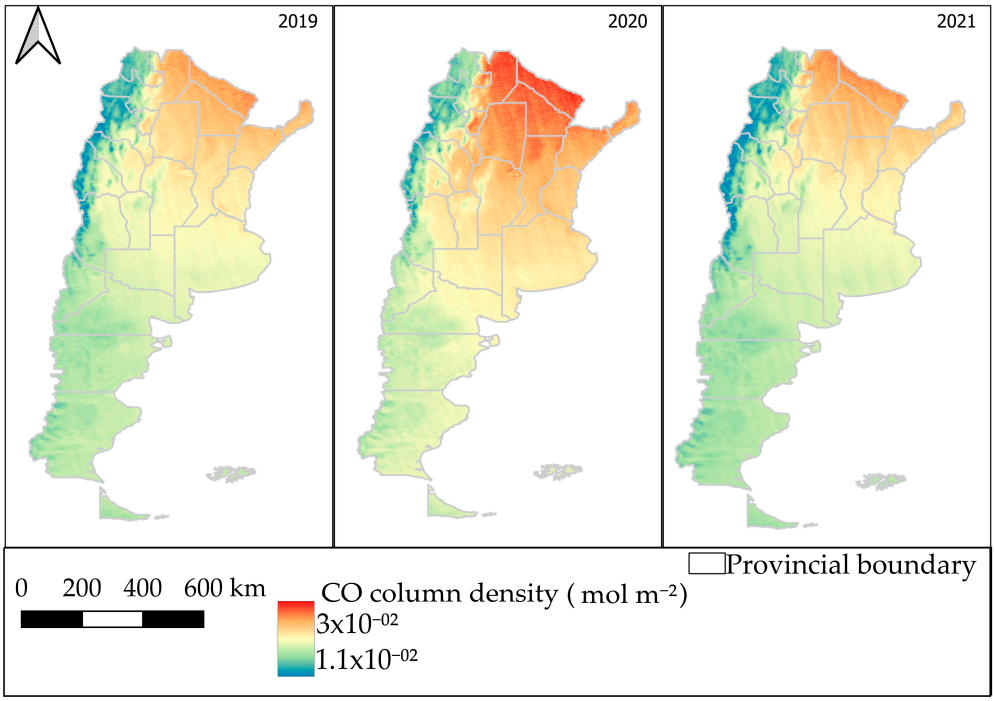


Figure 3. Annual maps of CO distribution (mol m^{-2}) for Argentina.

Regarding the spatial distribution of CO, the highest values were found in northeastern Argentina, coinciding with the areas of greatest vegetation cover such as the phytogeographic province Parque Chaqueño and with a high number of fires per year (Figure 3). Although southern Argentina also has forest cover such as the Andean-Patagonic forests, fires are less frequent [28,29]. Furthermore, the high CO concentrations in northern Argentina could be due to warm and humid climatic conditions compared with those in the south. These conditions favor the decomposition of organic matter and bacterial activity, which could result in the greater release of CO in forests. Finally, human activity such as agriculture, livestock, industrial, and vehicular traffic is more intense in the north of Argentina because it has a higher population density, which contributes to higher levels of CO in the air [30].

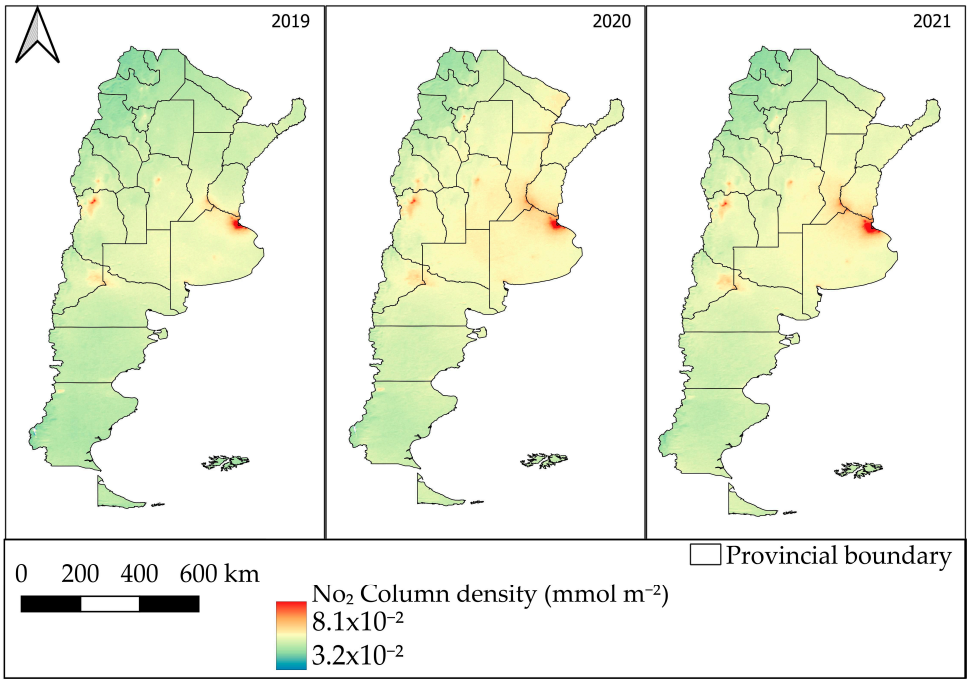


Figure 4. Annual maps of NO_2 distribution (mmol m^{-2}) for Argentina.

Table 1. Statistical parameters of CO and NO_2 gas concentrations for the different years of studies. These include maximum concentration (Max), average concentration, standard deviation (SD), and minimum concentration (Min) for Argentina.

		2019	2020	2021
CO (mol m^{-2})	Max	2.16×10^{-2}	2.99×10^{-2}	2.09×10^{-2}
	Mean	1.98×10^{-2}	2.13×10^{-2}	1.91×10^{-2}
	Sd	0.07×10^{-2}	0.34×10^{-2}	0.07×10^{-2}
	Min	1.70×10^{-2}	1.13×10^{-2}	1.64×10^{-2}
NO_2 (mmol m^{-2})	Max	7.71×10^{-2}	7.74×10^{-2}	8.13×10^{-2}
	Mean	5.14×10^{-2}	5.43×10^{-2}	5.35×10^{-2}
	Sd	0.33×10^{-2}	0.35×10^{-2}	0.35×10^{-2}
	Min	3.47×10^{-2}	3.22×10^{-2}	4.21×10^{-2}

Regarding NO_2 concentrations, the maximum values recorded increased from 2019 to 2021 (see Table 1). Figure 4 shows that the highest concentrations were found in the urban areas of Argentina. According to Gallardo et al. [9], NO_2 emissions are associated with high environment temperature and high oxygen content processes and occur mainly in the form of NO. In high-traffic urban areas, diesel vehicles can produce a significant contribution of NO_2. Also, the model showed a relationship between the NO_2 concentration and the interaction between explanatory area of the polygons and the class built-up land cover variables (estimate = 5.826×10^{-6}, p-value < 0.001), where the concentration of NO_2 began to be significant in an area greater than 6000 hectares for the urban class (Figure 5). This is the first work that demonstrates the minimum size of the urban area where NO_2 concentrations begin to be significant for the environment. The models with CO concentrations and the interaction between area and LULC did not show significant differences. This indicates that CO concentrations tended to remain in lower altitude areas of Argentina regions, such as valleys in mountainous areas or cities or natural areas close to sea level.

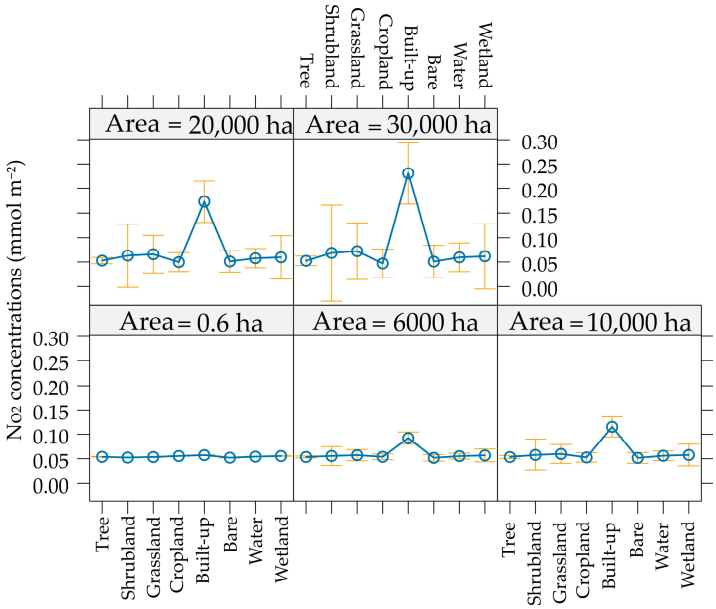


Figure 5. Generalized linear model (global model) explaining the variation in NO_2 concentration depending on the interaction between polygon area (ha) and LULC.

3.2. Influence of Land Uses and Land Cover on the Emission of CO and NO_2 over Time through Different Anthropic, Climatic, and Natural Indicators

GLMs were carried out to identify different anthropic, climatic, and natural indicators that affect the concentrations of CO and NO_2 in distinct LULC. Due to some uses and land covers having similar behavior in terms of the concentrations of these gases, the classes tree cover and herbaceous wetland, shrublands, grasslands, cropland, and built-up were grouped. The class bare/sparse vegetation was not grouped.

3.2.1. CO

The anthropic (national route, mining extraction) and climatic (Palmer drought index, vapor pressure, max environment temperature, and wind speed) variables explained 92% of the variability of CO concentrations in the tree cover/herbaceous wetland (Table 2). For the shrubland/grassland coverage, the anthropic (mining extraction, power plants, and airports), climatic (vapor pressure, max environment temperature, and wind speed), and natural (DEM and humidity) variables explained 96% of the variation in CO concentrations (Table 2). In the cropland/built-up coverage, the variation in CO concentrations was explained by the anthropic (mining extraction, power plants, and airports), climatic (vapor pressure and max environment temperature), and natural (DEM and NDVI) variables (50% of the variability). Finally, in the bare/sparse vegetation coverage, the mining extraction, IU (anthropic), vapor pressure, wind speed (climatic), and DEM (natural) variables explained 95.33% of the variation in CO concentration (Table 2).

In general, the variable distance from the mining extraction affected the CO concentrations independently of the type of land cover (Table 2), where the CO concentration increased as the distance to the mining extractions was smaller. This increase near mining companies is because the majority belong to crude oil extractions, which release volatile organic compounds in the process such as CO, CO_2, carbonic acid, ammonium carbonate, and carbonates. Oil production, exploration/extraction sites, and refineries are the second largest sources of volatile compounds after vehicle exhaust gases in the transportation sector [31]. This is because volatile compounds can escape from the oil mass during all stages of the crude oil industry [32].

Table 2. Generalized linear model (minimal adequate model) explaining the variation in the concentration of CO depending on anthropic, climatic, and natural indicators in the different LULC. The table shows the parameter estimates and their standard deviation (±SE), the *p*-values for significance (* = $p \leq 0.05$; ** = $p \leq 0.01$, *** = $p \leq 0.001$), and pseudo-R^2 for each model.

			CO		
LULC	**Type**	**Predictors**	**Estimate ± SE**	***p*-Value**	**Pseudo-R^2**
Tree cover/herbaceous wetland	Anthropic	National route	$-2.97 \times 10^{-9} \pm 1.49 \times 10^{-9}$	*	92.22
		Mining extraction	$-2.14 \times 10^{-9} \pm 2.81 \times 10^{-10}$	***	
	Climatic	Palmer drought index	$-1.50 \times 10^{-4} \pm 3.87 \times 10^{-5}$	***	
		Vapor pressure	$6.98 \times 10^{-3} \pm 4.33 \times 10^{-4}$	***	
		Max environment temperature	$1.16 \times 10^{-4} \pm 3.78 \times 10^{-5}$	**	
		Wind speed	$6.57 \times 10^{-4} \pm 9.16 \times 10^{-5}$	***	
Shrubland/grassland	Anthropic	Mining extraction	$-5.15 \times 10^{-10} \pm 1.90 \times 10^{-10}$	**	96.00
		Power plants	$-3.22 \times 10^{-9} \pm 1.39 \times 10^{-9}$	*	
		Airports	$-1.30 \times 10^{-9} \pm 6.70 \times 10^{-10}$	*	
	Climatic	Vapor pressure	$5.96 \times 10^{-3} \pm 3.09 \times 10^{-4}$	***	
		Max environment temperature	$1.52 \times 10^{-4} \pm 2.65 \times 10^{-5}$	***	
		Wind speed	$3.47 \times 10^{-4} \pm 5.40 \times 10^{-5}$	***	
	Natural	DEM	$-1.82 \times 10^{-7} \pm 7.65 \times 10^{-8}$	*	
		Humidity	$-2.95 \times 10^{-7} \pm 1.00 \times 10^{-7}$	**	
Cropland/built-up	Anthropic	National route	$-2.81 \times 10^{-9} \pm 1.61 \times 10^{-9}$	*	49.50
		Mining extraction	$-1.11 \times 10^{-9} \pm 2.90 \times 10^{-10}$	***	
	Climatic	Vapor pressure	$5.68 \times 10^{-3} \pm 4.33 \times 10^{-4}$	***	
		Max environment temperature	$1.63 \times 10^{-4} \pm 3.51 \times 10^{-5}$	***	
	Natural	DEM	$-4.07 \times 10^{-7} \pm 1.56 \times 10^{-7}$	**	
		NDVI	$-7.59 \times 10^{-4} \pm 4.04 \times 10^{-4}$	*	
Bare/sparse vegetation	Anthropic	Mining extraction	$-4.99 \times 10^{-10} \pm 2.19 \times 10^{-10}$	*	95.23
		IU	$8.61 \times 10^{-4} \pm 2.47 \times 10^{-4}$	***	
	Climatic	Vapor pressure	$6.68 \times 10^{-3} \pm 3.77 \times 10^{-4}$	***	
		Wind speed	$1.02 \times 10^{-4} \pm 4.80 \times 10^{-5}$	*	
	Natural	DEM	$-3.77 \times 10^{-7} \pm 6.65 \times 10^{-8}$	***	

The variable distance to the routes influenced tree cover/herbaceous wetland and cropland/built-up, where it could be observed that CO increased as the distance to the main routes decreased (Table 2). These results were expected in cropland/built-up coverage, where human activity was more intense [33]. However, the tree cover/herbaceous wetlands were also affected by the distances to the routes, concerning CO concentrations increasing as the distance to the routes decreased. This could be explained because the routes with the highest values of annual vehicular traffic are located in the northwest of the country, coinciding with the coverage of tree-cover/herbaceous wetlands (https://www.argentina.gob.ar/obras-publicas/vialidad-nacional/sig-vial (accessed on 15 November 2023)). Although sites with high vegetation cover are the main sinks of CO, probably when vehicular traffic is very intense, the vegetation cannot efficiently capture the CO emitted by the combustion of vehicles [34]. Additionally, the decomposition of organic matter, such as leaf litter and dead wood, can release CO as a byproduct of bacterial decomposition. In herbaceous wetlands, the anaerobic decomposition process of organic matter can also generate CO as a waste product. Microorganisms present in the swamp soil decompose organic matter under conditions of low oxygen availability, leading to the release of CO. In summary, in both forests and herbaceous wetlands, the decomposition of organic matter is an important source of CO, which can result in higher concentrations of this gas in the air [35]. While forests can also have CO emissions due to the decomposition

of organic matter, these levels tend to be lower compared with anthropogenic emissions in cities [36].

The distance to power plants and airports had a negative influence on shrubland/grassland coverage, since CO concentrations increased when the distance was smaller. Although shrubs and grasslands capture a CO percentage from the environment, power stations and airports generate a greater amount of CO released to the environment than these covers can sequester. Most of the garbage dumps in Argentina are open dumpsites, with some illegal and uncontrolled "landfills". Siddiqua et al. [37] found that landfilling was associated with various environmental pollutions, including air pollution due to the emissions of gases, which could cause illnesses in the exposed population living in their vicinity. Furthermore, the decomposition of organic materials in landfills produces different gases that have a composition of 50% CH_4, 50% CO_2, and a small amount of non-methane organic compounds [38,39]. Mining wastes and the difficulty of removal are very often sent for recovery or neutralization, whereas neutralization most often means disposal in dedicated landfills [40].

On the other hand, the results showed that CO concentration increased with the maximum environment temperature, wind speed, and vapor pressure in multiple land cover types (Table 2). As expected, high CO emissions into the atmosphere increased the environmental temperature, especially in cropland and built-up areas [41]. In natural areas such as tree cover, herbaceous wetlands, shrublands, and grasslands, CO emissions also increased, along with the environmental temperature. However, the Palmer index presented a negative relationship with the tree cover and herbaceous wetland. This indicated that, in extremely dry forests, the concentration of CO was greater. The increase in the environmental temperature, together with conditions of extreme drought, led to a greater predisposition to forest fires and consequently a greater emission of CO into the atmosphere. Finally, the CO concentrations presented a direct relationship with the rate of the winds in the different coverages. This indicated that CO concentrations moved through the atmosphere with the rate and direction of the winds. The natural variable (height (DEM)) negatively affected CO concentrations for shrublands and grasslands, croplands and built-up areas, and bare/sparse vegetation covers (Table 2). That is to say, CO concentrations increased with the altitude decrease, indicating that CO concentrations tended to remain in lower altitudes of Argentina areas, such as valleys in mountainous areas, cities, or natural areas close to sea level. However, a study in China showed simulation models that reported that, as urban land expands, the atmospheric load of CO and PM2.5 decreases near the surface (below km) but increases at higher altitudes (1 to 4 km) [42]. The humidity variable determined from the tasseled cap also negatively affected CO concentrations, but only in shrubland and grassland covers. This indicated that the lower the humidity of the bush and grassland vegetation the greater the CO concentration. Finally, the NDVI variable negatively affected CO concentrations for cropland and built-up areas. NDVI is an important phase indicator of terrestrial photosynthesis, which is usually used to analyze the CO_2 variation caused by vegetation [43]. Low NDVI values indicate areas with low coverage or impermeable surfaces such as cities, while values close to 1 indicate areas with vegetation such as cultivated areas. This work showed a gradual decrease in CO concentrations from urban to cultivated areas of the country.

3.2.2. NO_2

In relation to NO_2 concentrations, the percentage of variability explained through the GLM predictor variables was lower than for CO concentrations. The anthropic (airports, service stations), climatic (Palmer drought index), and natural (vapor pressure and DEM) variables explained 33.50% of the variability of NO_2 concentrations in the tree cover/herbaceous wetlands (Table 3). For the shrubland/grassland coverage, the open dumpsites and service stations (anthropic), Palmer drought index (climatic), and DEM (natural) variables explained 49.50% of the variation in NO_2 concentrations (Table 3). In the cropland/built-up coverage, the variation in NO_2 concentrations was explained by

the anthropic (power plants and open dumpsites), climatic (Palmer drought index), and natural (DEM) variables (33.34% of the variability). Finally, in the bare/sparse vegetation coverage, the factories/industry, wind speed, and DEM variables (anthropic, climatic, and natural, respectively) explained 57.02% of the variation in NO_2 concentration (Table 3).

Table 3. Generalized linear model (minimal adequate model) explaining the variation in the concentration of NO_2 depending on anthropic, climatic, and natural indicators in the different LULCs. The table shows the parameter estimates and their standard deviation (±SE), the *p*-values for significance (* = $p \leq 0.05$; ** = $p \leq 0.01$, *** = $p \leq 0.001$), and pseudo-R2 for each model.

			NO_2		
LULC	**Type**	**Predictors**	**Estimate ± SE**	***p*-Value**	**Pseudo-R^2**
Tree cover/herbaceous wetland	Anthropic	Airports	$-1.859 \times 10^{-8} \pm 6.240 \times 10^{-9}$	**	33.50
		Service stations	$-4.728 \times 10^{-8} \pm 1.423 \times 10^{-8}$	**	
	Climatic	Palmer drought index	$-9.309 \times 10^{-4} \pm 2.308 \times 10^{-4}$	***	
		Vapor pressure	$-2.873 \times 10^{-3} \pm 1.309 \times 10^{-3}$	*	
	Natural	DEM	$-4.749 \times 10^{-6} \pm 9.854 \times 10^{-7}$	***	
Shrubland/grassland	Anthropic	Open dumpsites	$-9.994 \times 10^{-9} \pm 1.386 \times 10^{-9}$	***	49.50
		Service stations	$-2.588 \times 10^{-8} \pm 6.302 \times 10^{-9}$	***	
	Climatic	Palmer drought index	$-2.182 \times 10^{-4} \pm 1.023 \times 10^{-4}$	*	
	Natural	DEM	$-1.385 \times 10^{-6} \pm 2.655 \times 10^{-7}$	***	
Cropland/built-up	Anthropic	Power plants	$-5.034 \times 10^{-8} \pm 1.363 \times 10^{-8}$	***	33.34
		Open dumpsites	$-2.238 \times 10^{-8} \pm 4.892 \times 10^{-9}$	***	
	Climatic	Palmer drought index	$-9.313 \times 10^{-4} \pm 2.927 \times 10^{-4}$	**	
	Natural	DEM	$-3.576 \times 10^{-6} \pm 1.037 \times 10^{-6}$	***	
Bare/sparse vegetation	Anthropic	Factories/industry	$-1.403 \times 10^{-6} \pm 1.901 \times 10^{-7}$	***	57.02
	Climatic	Wind speed	$-5.673 \times 10^{-4} \pm 1.200 \times 10^{-4}$	***	
	Natural	DEM	$-1.403 \times 10^{-6} \pm 1.901 \times 10^{-7}$	***	

It is accepted that NO_2 is not only a greenhouse gas but that it also contributes to ozone depletion in the stratosphere. However, it is much more reactive than CO_2 and therefore promotes combustion. NO_2 has an average residence time in the atmosphere of 170 years. At the current production rate, it is estimated that NO_2 concentrations will reach approximately 375 ppb per year.

In general, the urban variables that negatively affected the concentration of total NO_2 were open dumpsites, distance to power plants, service stations, airports, and factories/industry for the different LULCs. This indicated that the shorter the distance to the different urban variables, the higher the total NO_2 concentration (Table 3). The distance to the service stations harmed natural areas such as tree cover/herbaceous wetlands and shrubland/grassland coverage.

This indicates that NO_2 concentrations increased as the distance to gas stations decreased (Table 3). This finding is supported by previous studies that have shown that NO_2 emissions, mainly derived from vehicular traffic, can significantly increase in areas near gas stations [44]. Gas stations act as fuel refilling points and therefore attract a high volume of vehicular traffic. Previous studies have demonstrated that NO_2 emissions associated with traffic near service stations can contribute significantly to air pollution in urban and service stations [45]. Furthermore, NO_2 emissions may be more pronounced in areas near gas stations due to the higher number of vehicles that are in the process of stopping or accelerating when entering or leaving these facilities [46]. There is some concern about the different nitrogen oxides such as NO_2, N_2O, and NO released into the atmosphere by automobiles and other mobile sources [47]. In addition, this work demonstrated that the natural areas sampled did not reduce NO_2 concentrations around the service stations.

The covers of trees, herbaceous wetlands, and cropland/built-up presented an inverse relationship between NO_2 concentrations and distances to power plants. According to Puliafito et al. [48], air quality pollutants, such as NO_2 and SO_2, are mainly emitted by the transportation and energy sector. This is supported by previous research that has shown that NO_2 emissions from power plants can contribute significantly to local air pollution [49,50]. Power plants often burn coal, natural gas, or other fossil fuels to generate electricity, resulting in the release of air pollutants, including NO_2, as a byproduct of combustion [51]. Also, it was found that proximity to airports also had a negative effect on tree cover/herbaceous wetland coverage, indicating an increase in NO_2 concentrations at shorter distances from these sources (Table 3). Previous research found that airports, with their high concentration of aircraft and ground handling activities, can generate significant NO_2 emissions [50]. Riley et al. [52] also found high concentrations of NO_2 in the surroundings of airports. They stated that transportation within airports such as ground support equipment and motor vehicles contributed to increased NO_2 concentrations, and the increase in CO concentrations was primarily due to airplanes.

The "open dumpsites" variable also showed a negative effect on shrubland/grassland and cropland/built-up coverage, indicating that NO_2 concentrations increased at shorter distances from landfills or open dumpsites (Table 3). This aligns with the existing literature that has documented that the presence of landfills can be a significant source of NO_2 emissions due to the decomposition of organic waste and the release of pollutant gases [53]. Landfills are sites where large amounts of solid waste, including organic waste and decomposing materials, are deposited and accumulated. During the decomposition process, organic waste can release different gases, including NO_2, as a result of microbial activity. These emissions can be carried by the wind and dispersed in surrounding areas, resulting in higher concentrations of NO_2 in the air [53]. Furthermore, agricultural lands produce 8% of the emissions of different nitrogen oxides (NO_x) from the soil and should be the focus of efforts to improve estimates. The amount of NO_x emitted by these lands appears to be directly related to the nitrogen-based fertilizers applied to the soils and their subsequent nitrification and denitrification processing by soil bacteria [54]. Other agricultural practices, including burning and tillage, can increase NO_x emissions by a factor of 5 or more [55]. Soil NO_x emissions are also sensitive to soil temperature and soil moisture, which can be reasonably simulated using relatively simple algorithms [54,56]. Agriculture is the primary activity responsible for additional NO_2 emissions over the past century and a half. It is important to remark that, in rapeseed and corn (maize) crops (used to produce biodiesel and bioethanol), important quantities of nitrogen fertilizers are required. Thereby, NO_2 emissions could cause as much or more global warming as is avoided by substituting fossil fuels with biofuels. Therefore, it is important to avoid biofuel production based on crops with high nitrogen demand but to use those that can be grown with little or no fertilizer [57].

Finally, it was observed that the "factory/industry" variable harmed bare/sparse vegetation coverage, suggesting an increase in NO_2 concentrations at shorter distances from factories or industries (Table 3). Factories and industries are known to be significant sources of gas emissions, including NO_2, as a result of manufacturing processes and fuel combustion [58].

The climatic variables also influenced NO_2 concentrations across various land cover types. It was found that certain climatic factors had a significant impact on NO_2 concentrations, with notable effects observed on different types of vegetation covers. For NO_2, the climatic variables that influenced its concentration negatively were the Palmer index for tree cover, herbaceous wetland, shrubland, grassland, and cropland-built-up covers. In bare/sparse vegetation, the concentration of NO_2 was only influenced by wind speed. The Palmer index indicated that when drought increased, NO_2 increased as well (Table 3). This suggests that, in regions experiencing extreme drought, there was a greater accumulation of NO_2, possibly due to reduced atmospheric dispersion and increased emissions from various sources during dry periods. This finding was consistent with previous research

linking drought conditions to increased NO_2 levels [59]. Moreover, for bare/sparse vegetation cover, it was found that total NO_2 concentrations were solely influenced by wind rate. A negative relationship was observed between wind rate and NO_2 levels, implying that lower wind rates were associated with higher NO_2 concentrations (Table 3). This suggests that in areas devoid of significant vegetation, where surface roughness was low, wind rate became a critical factor governing the dispersion and concentration of NO_2. Previous studies have demonstrated the role of wind rate in dispersing pollutants and reducing their concentrations (see, [60]). In areas with calm wind conditions, NO_2 gases tended to accumulate more readily, exacerbating pollution levels in the atmosphere.

This study revealed a negative relationship between altitude (DEM) and NO_2 concentrations in all cover types (Table 3). This finding was consistent with previous research that highlighted the influence of altitude on the distribution of atmospheric pollutants [61]. It was observed that NO_2 concentrations tended to increase as altitude decreased, suggesting a greater accumulation of pollutants in lower altitude areas. One possible explanation for this phenomenon is the reduced atmospheric dispersion in lower-altitude areas, which may result in prolonged retention of pollutants in the atmosphere near the Earth's surface [62]. Additionally, NO_2 emission sources, such as vehicular traffic and industrial activities, tend to concentrate in urban and suburban areas, which are generally at lower altitudes.

4. Conclusions

This multi-temporal analysis has provided valuable insights into the dynamics of CO and NO_2 emissions in Argentina, elucidating their spatiotemporal distribution and the factors influencing their concentrations. The spatiotemporal distribution of CO and NO_2 in Argentina showed that their average concentrations were highest in 2020, showing lower values in 2019 and 2021. These results represent a novelty, since most research in different parts of the world have demonstrated that contaminant levels decreased during the isolation due to the COVID-19 pandemic. The spatial distribution of CO in Argentina indicated that the highest concentrations were found in northeastern regions with dense vegetation and higher population density, while southern regions had less frequent fires and lower CO levels. This study also revealed that NO_2 concentrations became significant in urban areas larger than 6000 hectares.

Furthermore, our study identified various factors influencing the concentrations of CO and NO_2 in different land cover types in Argentina. Proximity to mining extractions, main routes, power plants, and airports, as well as urbanization and natural variables such as environment temperature, wind rate, and altitude, all played a significant role in determining the levels of CO in the atmosphere. Additionally, human activities, such as waste disposal and organic matter decomposition, were highlighted as contributors to CO emissions, emphasizing the need for sustainable practices to mitigate air pollution in the region.

Similarly, numerous urban variables were found to significantly impact NO_2 concentrations, such as proximity to gas stations, power plants, airports, open dumpsites, and factories/industries, leading to increased levels. Climatic factors such as wind rate and drought, as well as altitude and vegetation density, played crucial roles in influencing NO_2 concentrations across different land cover types, emphasizing the complex interplay between urban, climatic, and environmental factors in determining air quality.

This study underscores the crucial role that LULC in shaping the environmental conditions of a region. Understanding the dynamics of these factors and their impact on emissions of harmful pollutants, such as nitrogen dioxides and carbon monoxide (CO), is essential for effective environmental management. The results reported in this study will be of interest to those concerned with the development of effective strategies to mitigate pollution levels such as researchers and government entities that must make decisions about the environment and its sustainability.

While this study has provided valuable insights into the dynamics of CO and NO_2 emissions in Argentina, additional research avenues exist to deepen the understanding and

inform future mitigation efforts. Considering temporal variations, policy impacts, long-term trends, technological advancements, community engagement, and health implications will be essential for effective environmental management and safeguarding public health in Argentina.

Author Contributions: Conceptualization, V.F.-M., A.L.N. and M.P.F.; methodology, V.F.-M., A.L.N., R.R. and M.P.F.; software, V.F.-M.; formal analysis, V.F.-M.; investigation, V.F.-M. and A.L.N.; resources, V.F.-M. and R.R.; writing—original draft preparation, V.F.-M. and A.L.N.; writing—review and editing, A.L.N., R.R. and G.M.; visualization, R.R.; supervision, R.R.; funding acquisition, V.F.-M. and R.R. All authors have read and agreed to the published version of the manuscript.

Funding: The authors wish to thank the support of the following Argentine institutions: the University of San Juan (PDTS I1471 y E1245 Res.1499/23); the University of Comahue (PIN 2022-04/I260); CONICET—National Scientific and Technical Research Council (PIP 2021–2023—11220200100950CO); ANPCYT-FONCYT (PICT 2019-01810); FONCYT-PICTA RESOL-2022-87 Project Number 20 (2022). Viviana Fernandez, Ana Laura Navas, Paula Fabani, Rosa Rodriguez, and Germán Mazza are Research Members of CONICET, Argentina.

Institutional Review Board Statement: Not applicable.

Informed Consent Statement: Not applicable.

Data Availability Statement: The data presented in this study are available on request from the corresponding author.

Acknowledgments: We thank the National Scientific and Technical Research Council of Argentina (CONICET) and the National University of San Juan for providing us with their support and physical space to carry out the research.

Conflicts of Interest: The authors declare no conflicts of interest.

Appendix A

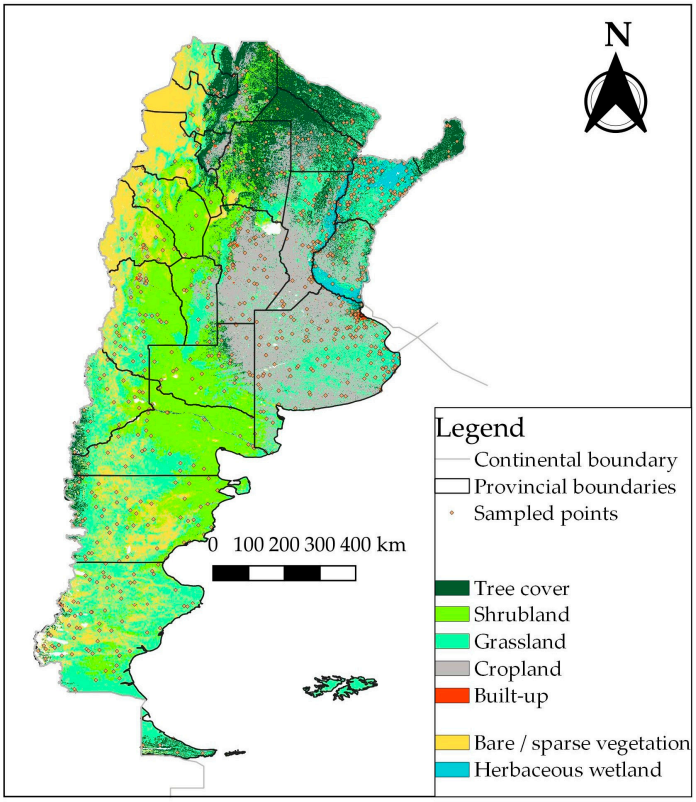


Figure A1. Map showing the different LULCs and the sampling points for each coverage.

```
Model 1< -glm(response variable~predictor variable1+predictor variable2+…,data=table,
family= Gamma(link = "identity"))
summary(Model1)
par(mfrow=c(2,2))
plot(Model1)
par(mfrow=c(1,1))
```

Figure A2. The following figure describes the script detailing the formula used in gamma models in the R program.

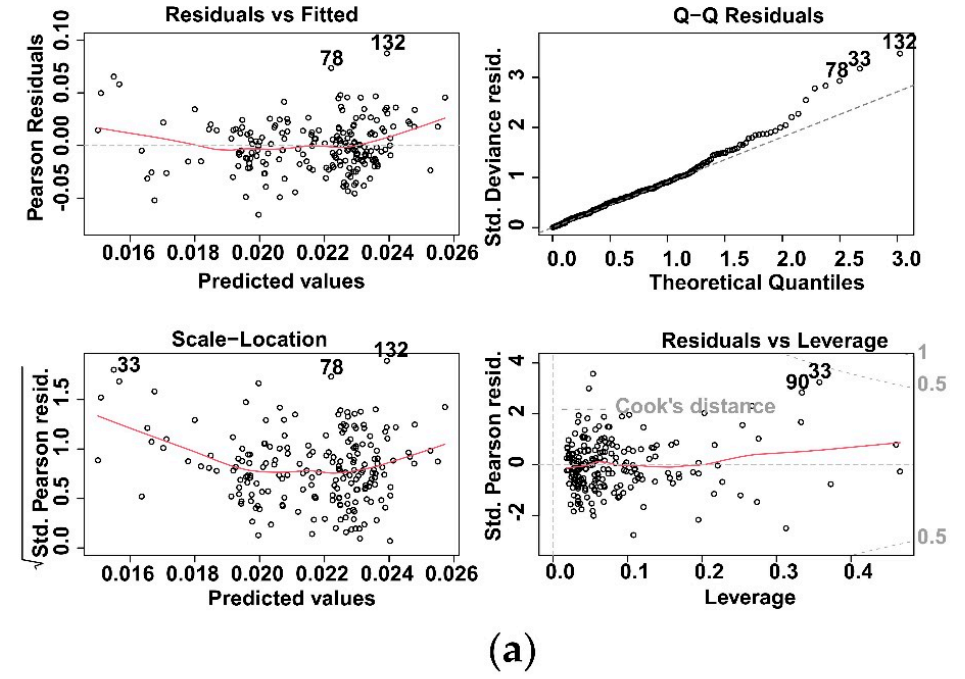


Figure A3. Fitting the GLM with gamma distribution for tree cover/herbaceous wetland for both gases (**a**) CO and (**b**) NO_2.

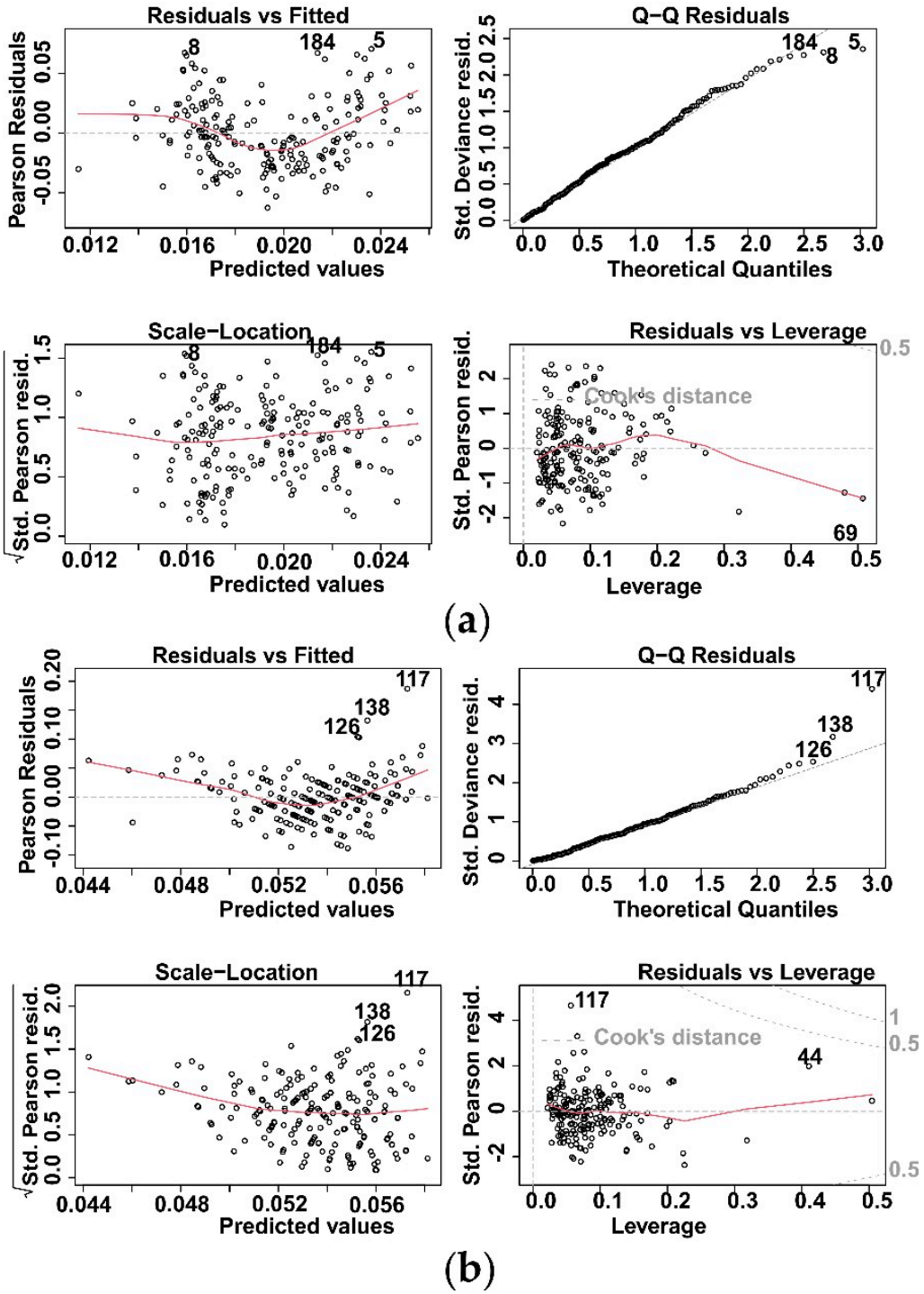


Figure A4. Fitting the GLM with gamma distribution for shrubland/grassland coverage for both gases (**a**) CO and (**b**) NO_2.

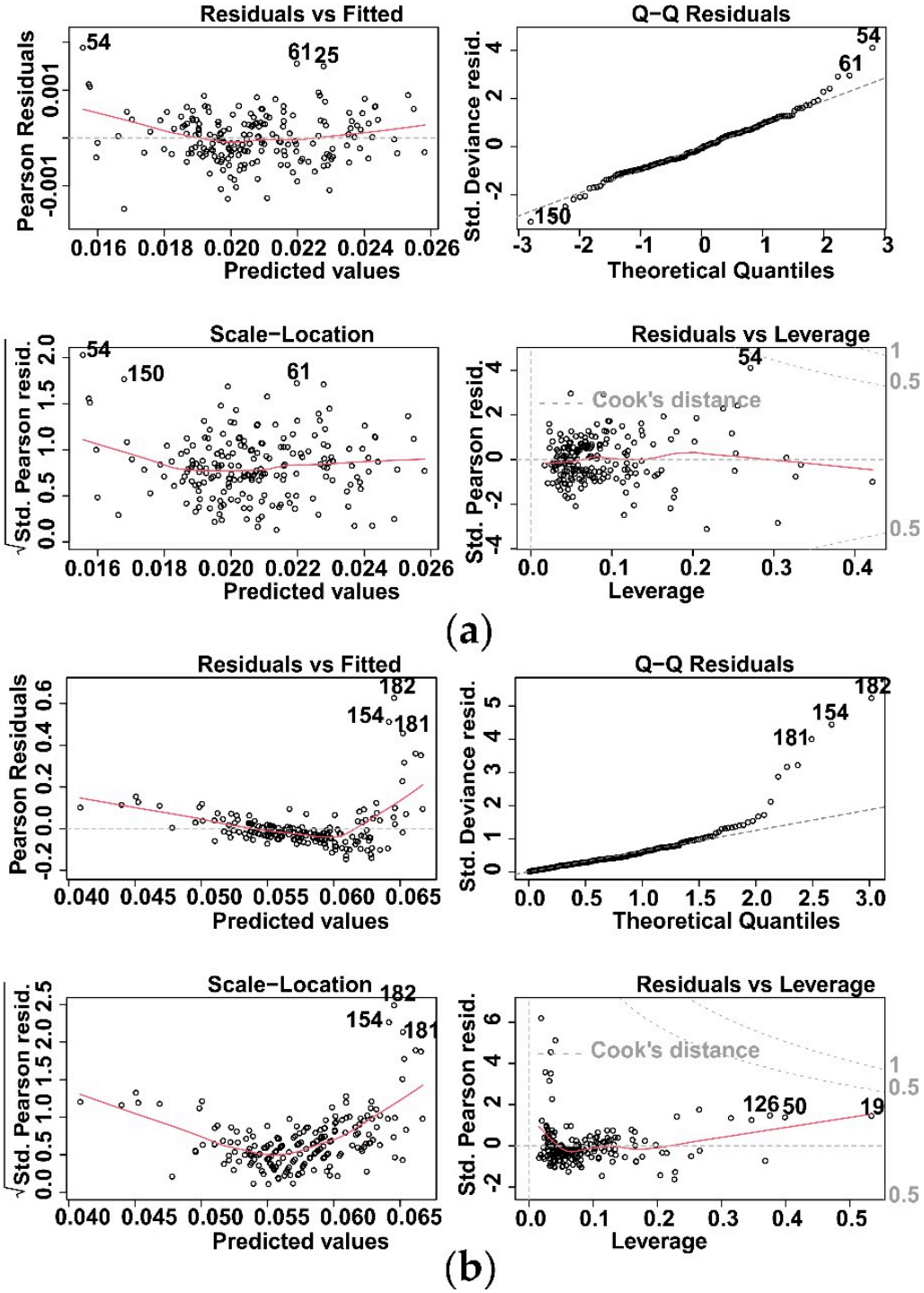


Figure A5. Fitting the GLM with gamma distribution for cropland/built-up coverage for both gases (**a**) CO and (**b**) NO_2.

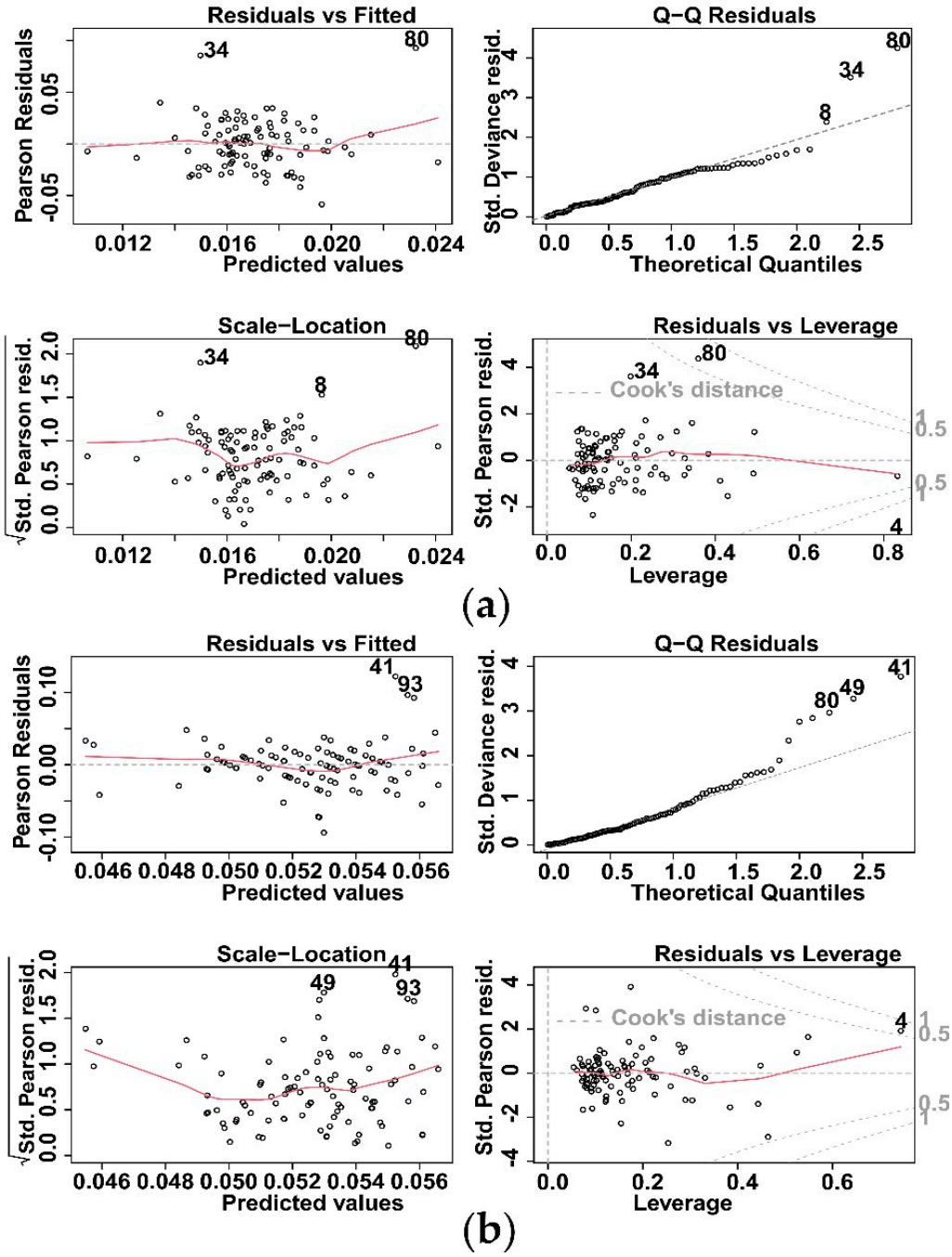


Figure A6. Fitting the GLM with gamma distribution for bare/sparse vegetation coverage for both gases (**a**) CO and (**b**) NO_2.

References

1. Rafaj, P.; Kiesewetter, G.; Gül, T.; Schöpp, W.; Cofala, J.; Klimont, Z.; Purohit, P.; Heyes, C.; Amann, M.; Borken-Kleefeld, J.; et al. Outlook for clean air in the context of sustainable development goals. *Glob. Environ. Chang.* **2018**, *53*, 1–11. [CrossRef]
2. Mannucci, P.M.; Franchini, M. Health effects of ambient air pollution in developing countries. *Int. J. Environ. Res. Public Health* **2017**, *14*, 1048. [CrossRef] [PubMed]
3. Cohen, A.J.; Brauer, M.; Burnett, R.; Anderson, H.R.; Frostad, J.; Estep, K.; Forouzanfar, M.H. Estimates and 25-year trends of the global burden of disease attributable to ambient air pollution: An analysis of data from the Global Burden of Diseases Study 2015. *Lancet* **2017**, *389*, 1907–1918. [CrossRef] [PubMed]
4. WHO. Burden of Disease from Ambient Air Pollution for 2016. In *Technical Report, World Health Organization, Version 2*; WHO: Geneva, Switzerland, 2018. Available online: https://cdn.who.int/media/docs/default-source/air-pollution-documents/air-quality-and-health/aap_bod_results_may2018_final.pdf (accessed on 4 January 2021).

5. WHO. *Health Effects of Particulate Matter*; World Health Organization, WHO Regional Office for Europe: Copenhagen, Denmark, 2020. Available online: https://unece.org/DAM/env/documents/2013/air/Health-effects-of-particulate-matter-final-Eng.pdf (accessed on 5 January 2021).
6. Manisalidis, I.; Stavropoulou, E.; Stavropoulos, A.; Bezirtzoglou, E. Environmental and health impacts of air pollution: A review. *Front. Public Health* **2020**, *8*, 505570. [CrossRef] [PubMed]
7. Tito, A.; Messan, F.; Togbenou, K.; Bio Nigan, I.; Dosseh, K. Toxicological responses of Wistar rats exposed to controlled emissions of carbon monoxide and nitrogen dioxide. *WJRR* **2019**, *8*, 09–15. [CrossRef]
8. Shikwambana, L.; Mhangara, P.; Mbatha, N. Trend analysis and first-time observations of sulphur dioxide and nitrogen dioxide in Southafrica using TROPOMI/Sentinel-5 P data. *Int. J. Appl. Earth Obs. Geoinf.* **2020**, *91*, 102130. [CrossRef]
9. Gallardo, L.; Escribano, J.; Dawidowski, L.; Rojas, N.; de Fátima Andrade, M.; Osses, M. Evaluation of vehicle emission inventories for carbon monoxide and nitrogen oxides for Bogotá, Buenos Aires, Santiago, and São Paulo. *Atmos. Environ.* **2012**, *47*, 12–19. [CrossRef]
10. Yarragunta, Y.; Srivastava, S.; Mitra, D.; Chandola, H.C. Influence of forest fire episodes on the distribution of gaseous air pollutants over Uttarakhand, India. *GIScience Remote Sens.* **2020**, *57*, 190–206. [CrossRef]
11. Olorunfemi, I.E.; Fasinmirin, J.T.; Olufayo, A.A.; Komolafe, A.A. GIS and remote sensing-based analysis of the impacts of land use/land cover change (LULCC) on the environmental sustainability of Ekiti State, southwestern Nigeria. *Environ. Dev. Sustain.* **2020**, *22*, 661–692. [CrossRef]
12. Fernandez Maldonado, V.N.; Gatica, G.; Cardús Monserrat, A.L.; Campos, V.E. Evaluación de los cambios en el uso y cobertura del suelo en una ciudad en desarrollo basado en imágenes satelitales. *Rev. Geogr.* **2023**, *26*, 4–14.
13. Zhong, C.; Guo, H.; Swan, I.; Gao, P.; Yao, Q.; Li, H. Evaluating trends, profits, and risks of global cities in recent urban expansion for advancing sustainable development. *Habitat Int.* **2023**, *138*, 102869. [CrossRef]
14. Jiang, H.; Sun, Z.; Guo, H.; Weng, Q.; Du, W.; Xing, Q.; Cai, G. An assessment of urbanization sustainability in China between 1990 and 2015 using land use efficiency indicators. *Npj Urban Sustain.* **2021**, *1*, 34. [CrossRef]
15. Le, T.; Wang, Y.; Liu, L.; Yang, J.; Yung, Y.L.; Li, G.; Seinfeld, J.H. Unexpected air pollution with marked emission reductions during the COVID-19 outbreak in China. *Science* **2020**, *369*, 702–706. [CrossRef] [PubMed]
16. Ooi, M.C.G.; Chan, A.; Ashfold, M.J.; Oozeer, M.Y.; Morris, K.I.; Kong, S.S.K. The role of land use on the local climate and air quality during calm inter-monsoon in a tropical city. *Geosci. Front.* **2019**, *10*, 405–415. [CrossRef]
17. Veefkind, J.; Aben, I.; McMullan, K.; Forster, H.; de Vries, J.; Otter, G.; Claas, J.; Eskes, H.; de Haan, J.; Kleipool, Q.; et al. TROPOMI on the ESA Sentinel-5 Precursor: A GMES mission for global observations of the atmospheric composition for climate, air quality and ozone layer applications. *Rem. Sens. Environ.* **2012**, *120*, 70–83. [CrossRef]
18. Zha, Y.; Gao, J.; Ni, S. Use of normalized difference built-up index in automatically mapping urban areas from TM imagery. *Int. J. Remote Sens.* **2003**, *24*, 583–594. [CrossRef]
19. Montero, D.; Aybar, C.; Mahecha, M.D.; Martinuzzi, F.; Söchting, M.; Wieneke, S. A standardized catalogue of spectral indices to advance the use of remote sensing in Earth system research. *Sci. Data* **2023**, *10*, 197. [CrossRef]
20. Abatzoglou, J.T.; Dobrowski, S.Z.; Parks, S.A.; Hegewisch, K.C. TerraClimate, a high-resolution global dataset of monthly climate and climatic water balance from 1958–2015. *Sci. Data* **2018**, *5*, 170191. [CrossRef] [PubMed]
21. Heiberger, R.M.; Holland, B. *Statistical Analysis and Data Display: An Intermediate Course with Examples in S-Plus, R, and SAS*, 2nd ed.; Springer: New York, NY, USA, 2009; pp. 263–314.
22. Crawley, M.J. *The R Book*, 2nd ed.; Wiley: Sussex, UK, 2013; pp. 388–448.
23. Zuur, A.F.; Ieno, E.N.; Walker, N.J.; Saveliev, A.A.; Smith, G.M. Mixed effects models and extensions in ecology with R. In *Springer Science*; Springer: Berlin/Heidelberg, Germany, 2009. [CrossRef]
24. Zar, J. *Biostatistical Analysis*, 5th ed.; Pearson Prentice Hall: Upper Saddle River, NJ, USA, 1999.
25. Muniraj, K.; Panneerselvam, B.; Devaraj, S.; Jesudhas, C.J.; Sudalaimuthu, K. Evaluating the effectiveness of emissions reduction measures and ambient air quality variability through ground-based and Sentinel-5P observations under the auspices of COVID pandemic lockdown in Tamil Nadu, India. *Int. J. Environ. Anal. Chem.* **2023**, *103*, 3109–3120. [CrossRef]
26. Shami, S.; Ranjgar, B.; Bian, J.; Khoshlahjeh Azar, M.; Moghimi, A.; Amani, M.; Naboureh, A. Trends of CO and NO_2 Pollutants in Iran during COVID-19 pandemic using Timeseries Sentinel-5 images in Google Earth Engine. *Pollutants* **2022**, *2*, 156–171. [CrossRef]
27. Gharbia, R.; Hassanien, A.E. Carbon monoxide air pollution monitoring approach in Africa during COVID-19 pandemic. In *The Global Environmental Effects During and Beyond COVID-19: Intelligent Computing Solutions*; Springer: Berlin/Heidelberg, Germany, 2021; pp. 93–103.
28. Veraverbeke, S.; Sedano, F.; Hook, S.J.; Randerson, J.T.; Jin, Y.; Rogers, B.M. Mapping the daily progression of large wildland fires using MODIS active fire data. *Int. J. Wildland Fire* **2014**, *23*, 655–667. [CrossRef]
29. Carretero, E.M. Los incendios forestales en la Argentina. *Multequina* **1995**, *4*, 105–114.
30. Ginzo, H.D. Emisiones de gases de efecto invernadero y mitigación en el sector de uso del suelo, cambio en el uso del suelo y silvicultura: Economía del cambio climático en la Argentina. *Ser. Medio Ambiente y Desarro.* **2015**, *160*, 1–44.
31. Rajabi, H.; Mosleh, M.H.; Mandal, P.; Lea-Langton, A.; Sedighi, M. Emissions of volatile organic compounds from crude oil processing–Global emission inventory and environmental release. *Sci. Total Environ.* **2020**, *727*, 138654. [CrossRef]

32. Warneke, C.; Geiger, F.; Edwards, P.M.; Dube, W.; Pétron, G.; Kofler, J.; Zahn, A.; Brown, S.S.; Graus, M.; Gilman, J.B.; et al. Volatile Organic Compound Emissions from the Oil and Natural Gas Industry in the Uintah Basin, Utah: Oil and Gas Well Pad Emissions Compared to Ambient Air Composition. *Atmos. Chem. Phys.* **2014**, *14*, 10977–10988. [CrossRef]
33. Zalzal, J.; Alameddine, I.; El-Fadel, M.; Weichenthal, S.; Hatzopoulou, M. Drivers of seasonal and annual air pollution exposure in a complex urban environment with multiple source contributions. *Environ. Monit. Assess.* **2020**, *192*, 415. [CrossRef]
34. Sha, Z.; Bai, Y.; Li, R.; Lan, H.; Zhang, X.; Li, J.; Lan, H.; Zhang, X.; Li, J.; Liu, X.; et al. The global carbon sink potential of terrestrial vegetation can be increased substantially by optimal land management. *Commun. Earth Environ.* **2022**, *3*, 8. [CrossRef]
35. Bian, H.; Zheng, S.; Liu, Y.; Xu, L.; Chen, Z.; He, N. Changes to soil organic matter decomposition rate and its temperature sensitivity along water table gradients in cold-temperate forest swamps. *Catena* **2020**, *194*, 104684. [CrossRef]
36. Mäkipää, R.; Abramoff, R.; Adamczyk, B.; Baldy, V.; Biryol, C.; Bosela, M.; Lehtonen, A. How does management affect soil C sequestration and greenhouse gas fluxes in boreal and temperate forests?—A review. *For. Ecol. Manag.* **2023**, *529*, 120637. [CrossRef]
37. Siddiqua, A.; Hahladakis, J.N.; Al-Attiya, W.A.K. An overview of the environmental pollution and health effects associated with waste landfilling and open dumping. *Environ. Sci. Pollut. Res.* **2022**, *29*, 58514–58536. [CrossRef]
38. Yaashikaa, P.R.; Kumar, P.S.; Nhung, T.C.; Hemavathy, R.V.; Jawahar, M.J.; Neshaanthini, J.P.; Rangasamy, G. A review on landfill system for municipal solid wastes: Insight into leachate, gas emissions, environmental and economic analysis. *Chemosphere* **2022**, *309*, 136627. [CrossRef]
39. Andriani, D.; Atmaja, T.D. The potentials of landfill gas production: A review on municipal solid waste management in Indonesia. *J. Mater. Cycles Waste Manag.* **2019**, *21*, 1572–1586. [CrossRef]
40. Kalisz, S.; Kibort, K.; Mioduska, J.; Lieder, M.; Małachowska, A. Waste management in the mining industry of metals ores, coal, oil and natural gas-A review. *J. Environ. Manag.* **2022**, *304*, 114239. [CrossRef]
41. Pongratz, J.; Schwingshackl, C.; Bultan, S.; Obermeier, W.; Havermann, F.; Guo, S. Land use effects on climate: Current state, recent progress, and emerging topics. *Curr. Clim. Change Rep.* **2021**, *7*, 99–120. [CrossRef]
42. Tao, W.; Liu, J.; Ban-Weiss, G.A.; Hauglustaine, D.A.; Zhang, L.; Zhang, Q.; Tao, S. Effects of urban land expansion on the regional meteorology and air quality of eastern China. *Atmos. Chem. Phys.* **2015**, *15*, 8597–8614. [CrossRef]
43. Duan, Z.; Yang, Y.; Wang, L.; Liu, C.; Fan, S.; Chen, C.; Gao, Z. Temporal characteristics of carbon dioxide and ozone over a rural-cropland area in the Yangtze River Delta of eastern China. *Sci. Total Environ.* **2021**, *757*, 143750. [CrossRef]
44. Smith, L.; Mukherjee, S.; Kovalcik, K.; Sams, E.; Stallings, C.; Hudgens, E.; Neas, L. Near-road measurements for nitrogen dioxide and its association with traffic exposure zones. *Atmos. Pollut. Res.* **2015**, *6*, 1082–1086. [CrossRef]
45. Wheeler, A.J.; Smith-Doiron, M.; Xu, X.; Gilbert, N.L.; Brook, J.R. Intra-urban variability of air pollution in Windsor, Ontario—Measurement and modeling for human exposure assessment. *Environ. Res.* **2008**, *106*, 7–16. [CrossRef]
46. Yu, K.A.; McDonald, B.C.; Harley, R.A. Evaluation of nitrogen oxide emission inventories and trends for on-road gasoline and diesel vehicles. *Environ. Sci. Technol.* **2021**, *55*, 6655–6664. [CrossRef]
47. Clairotte, M.; Suarez-Bertoa, R.; Zardini, A.A.; Giechaskiel, B.; Pavlovic, J.; Valverde, V.; Ciufo, B.; Astorga, C. Exhaust emission factors of greenhouse gases (GHGs) from European road vehicles. *Environ. Sci. Eur.* **2020**, *32*, 125. [CrossRef]
48. Puliafito, S.E.; Bolaño-Ortiz, T.R.; Pena, L.L.B.; Pascual-Flores, R.M. Dataset supporting the estimation and analysis of high spatial resolution inventories of atmospheric emissions from several sectors in Argentina. *Data Brief* **2020**, *29*, 105281. [CrossRef]
49. Liu, F.; Duncan, B.N.; Krotkov, N.A.; Lamsal, L.N.; Beirle, S.; Griffin, D.; McLinden, C.A.; Goldberg, D.L.; Lu, Z. A methodology to constrain carbon dioxide emissions from coal-fired power plants using satellite observations of co-emitted nitrogen dioxide. *Atmos. Chem. Phys.* **2020**, *20*, 99–116. [CrossRef]
50. Guzmán, P.; Tarín-Carrasco, P.; Morales-Suárez-Varela, M.; Jiménez-Guerrero, P. Effects of air pollution on dementia over Europe for present and future climate change scenarios. *Environ. Res.* **2022**, *204*, 112012. [CrossRef]
51. Filonchyk, M.; Peterson, M.P. An integrated analysis of air pollution from US coal-fired power plants. *Geosci. Front.* **2023**, *14*, 101498. [CrossRef]
52. Riley, K.; Cook, R.; Carr, E.; Manning, B. A systematic review of the impact of commercial aircraft activity on air quality near airports. *City Environ. Interact.* **2021**, *11*, 100066. [CrossRef]
53. Lee, N.H.; Song, S.H.; Jung, M.J.; Kim, R.H.; Park, J.K. Dynamic emissions of N2O from solid waste landfills: A review. *Environ. Eng. Res.* **2023**, *28*, 220630. [CrossRef]
54. Skiba, U.; Medinets, S.; Cardenas, L.M.; Carnell, E.J.; Hutchings, N.J.; Amon, B. Assessing the contribution of soil NO_x emissions to European atmospheric pollution. *Environ. Res. Lett.* **2021**, *16*, 025009. [CrossRef]
55. Civerolo, K.L.; Dickerson, R.R. Nitric oxide soil emissions from tilled and untilled cornfields. *Agric. For. Meteorol.* **1998**, *90*, 307–311. [CrossRef]
56. Yienger, J.J.; Levy, H. Empirical model of global soil-biogenic NO_x emissions. *J. Geophys. Res. Atmos.* **1995**, *100*, 11447–11464. [CrossRef]
57. Lazcano, C.; Zhu-Barker, X.; Decock, C. Effects of organic fertilizers on the soil microorganisms responsible for N_2O emissions: A review. *Microorganisms* **2021**, *9*, 983. [CrossRef]
58. Novikov, A.V.; Shiryaeva, M.A.; Sumarukova, O.V.; Lagutina, N.V.; Barsukova, M.V. Impact factory assessment on the air on the Pekhorka river basin. *IOP Conf. Ser. Earth Environ. Sci.* **2021**, *723*, 052005. [CrossRef]

59. Zheng, Z.; Yang, Z.; Wu, Z.; Marinello, F. Spatial variation of NO_2 and its impact factors in China: An application of sentinel-5P products. *Remote Sens.* **2019**, *11*, 1939. [CrossRef]
60. Zhou, Y.; Levy, J.I. Factors influencing the spatial extent of mobile source air pollution impacts: A meta-analysis. *BMC Public Health* **2007**, *7*, 1939. [CrossRef]
61. Lu, X.; Cao, L.; Ding, H.; Gao, M.; Meng, X. The relationship between the altitude and the simulations of ozone and NO_2 by WRF-Chem for the Tibetan Plateau. *Atmos. Environ.* **2022**, *274*, 118981. [CrossRef]
62. Zhao, P.; Liu, J.; Luo, Y.; Wang, X.; Li, B.; Xiao, H.; Zhou, Y. Comparative analysis of long-term variation characteristics of SO_2, NO_2, and O_3 in the ecological and economic zones of the Western Sichuan plateau, Southwest China. *Int. J. Environ. Res. Public Health* **2019**, *16*, 3265. [CrossRef]

Disclaimer/Publisher's Note: The statements, opinions and data contained in all publications are solely those of the individual author(s) and contributor(s) and not of MDPI and/or the editor(s). MDPI and/or the editor(s) disclaim responsibility for any injury to people or property resulting from any ideas, methods, instructions or products referred to in the content.